Globular clusters and the evolution of their multiple stellar populations

W. Chantereau[1], C. Charbonnel[1,2] and G. Meynet[1]

[1]Department of Astronomy, University of Geneva,
Chemin des Maillettes 51, CH-1290 Versoix, Switzerland
email: william.chantereau@unige.ch

[2]RAP, UMR 5277 CNRS and Université de Toulouse,
14 Av. E. Belin, F-31400 Toulouse, France

Abstract. Our knowledge of the formation and early evolution of globular clusters (GCs) has been totally shaken with the discovery of the peculiar chemical properties of their long-lived host stars. Therefore, the interpretation of the observed Colour Magnitude Diagrams (CMD) and of the properties of the GC stellar populations requires the use of new stellar models computed with relevant chemical compositions. In this paper we use the grid of evolution models for low-mass stars computed by Chantereau *et al.* (2015) with the initial compositions of second-generation stars as predicted by the fast rotating massive stars scenario to build synthesis models of GCs. We discuss the implications of the assumed initial chemical distribution on 13 Gyr isochrones. We build population synthesis models to predict the fraction of stars born with various helium abundances in present day globular clusters (assuming an age of 13 Gyr). With the current assumptions, 61 % of stars on the main sequence are predicted to be born with a helium abundance in mass fraction, Y_{ini}, smaller than 0.3 and only 11 % have a Y_{ini} larger than 0.4. Along the horizontal branch, the fraction of stars with Y_{ini} inferior to 0.3 is similar to that obtained along the main sequence band (63 %), while the fraction of very He-enriched stars is significantly decreased (only 3 % with Y_{ini} larger than 0.38).

Keywords. globular clusters: general, Hertzsprung-Russell diagram, stars: evolution, stars: low-mass, stars: abundances

1. Introduction

It is now well accepted that GCs host at least two populations of low-mass stars, one presenting the chemical patterns typical of the protoglobular cluster gas and of halo stars of similar metallicity (first population, 1P), while the other one displays peculiar abundances (second population, 2P). This overall picture has been set up thanks to numerous spectroscopic surveys (see e.g. Gratton *et al.* 2001; Carretta *et al.* 2009a, 2009b), and the famous O-Na anti-correlation has been adopted as the main characteristic of a *bona-fide* GC (Carretta *et al.* 2010). In addition, with the advent of high resolution photometry, this paradigm has been strongly supported by the discovery of multiple discrete structures in CMDs of individual GCs (see e.g. Bedin *et al.* 2004; Piotto *et al.* 2007; Piotto 2009; Milone *et al.* 2013). Different scenarios implying different polluters have been developed to explain the nucleosynthetic sources of ashes of H-burning at high temperature needed to explain the chemical composition of 2P stars. The main polluters advocated in the literature are fast rotating massive stars (FRMS, Decressin *et al.* 2007; Krause *et al.* 2013), asymptotic giant branch stars (AGB, Ventura *et al.* 2001, 2013), massive binary stars (de Mink *et al.* 2009), supermassive stars (Denissenkov & Hartwick 2014), and also low-mass pre-main sequence stars coupled with interactive binaries/and or rotating massive stars (Bastian *et al.* 2013).
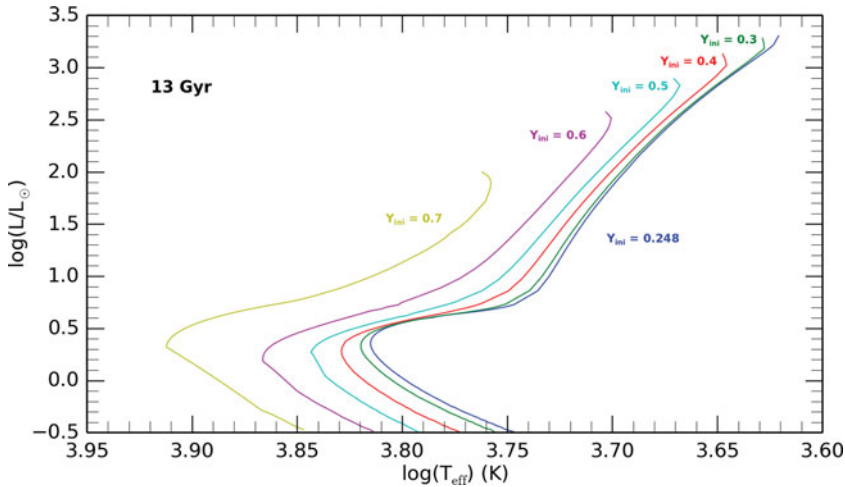
Figure 1. Theoretical isochrones at 13 Gyr for different initial helium composition between 0.248 and 0.7 (mass fraction).

Despite the numerous differences between the scenarios developed to explain the typical chemical patterns of GCs, it is widely accepted by the community that 2P stars have formed with a higher helium content than their 1P counterparts. It is then mandatory to take into account the impact of various helium content on the evolution of stars in order to provide a fully consistent scenario. Each of the above scenarios predict different initial helium content in the 2P stars. The various initial He distributions associated will then evolve into different distributions as a result of the evolution of stars and give therefore various outcomes for the helium distribution in the present day GCs. This is the point that we study in the present paper. More specifically, we start from the initial abundances predicted by the FRMS scenario and we predict the helium distribution that one should observe in the cluster NGC 6752. Although helium abundances remain very difficult to measure directly by spectroscopy in cool stars, there exist indirect ways to constrain the present day helium distribution in GCs (see e.g. Salaris *et al.* 2004).

2. General framework

In the FRMS scenario, 2P stars form in the immediate vicinity of very massive and fast rotating stars (into the mass range 25-120 $M_\odot$ as investigated by Decressin *et al.* 2007a,b; Krause *et al.* 2013) from their H-burning ashes diluted at various degrees with the surrounding intra-cluster pristine gas. Therefore 2P stars are mainly C-, O-, and Mg-depleted while they are He-, N-, Na-, and Al-enriched, compared to their 1P counterparts that display a chemical composition typical of the pristine intra-cluster material and of the surrounding halo field stars. At the metallicity investigated in this study ([Fe/H] = -1.75), 2P stars are expected to be born with $Y_{\rm ini}$ ranging between 0.248 (as 1P) and 0.8.

3. Isochrones

Stellar models enriched in helium have a higher luminosity and effective temperature ($T_{\rm eff}$), thus evolve faster (see Chantereau *et al.* (2015), hereafter paper I, for more details). At a given age, He-enriched isochrones are thus located in the HRD at a higher $T_{\rm eff}$, and are populated by lower masses than the reference isochrone ($Y_{\rm ini} = 0.248$, see fig. 1).

More quantitatively, the effective temperature of stars with a solar luminosity are hotter by 1,400 K when their initial helium abundance is 0.7 instead of 0.248. At this luminosity, the 2P stars with $Y_{ini} = 0.7$ display a mass lower by $\sim 0.4\ M_\odot$ than their 1P counterparts. These differences are much smaller for models moderately enriched in helium, still at solar luminosity, we expect 'only' an increase of less than ~ 100 K between the reference isochrone and the $Y_{ini} = 0.3$ one, which is similar to the error in T_{eff}. Along the RGB, we expect the same behaviour for the He-rich models as for the previous phase, i.e. mainly an increase of the T_{eff} with the helium enhancement. This time the dispersion is smaller than the one at solar luminosity, slightly above 700 K for the $Y_{ini} = 0.7$ case in the middle of the RGB ($\log(L/L_\odot) = 1.5$). Again, for lower helium enrichments (e.g. $Y_{ini} = 0.4$), the increase in T_{eff} is only ~ 100 K. Finally, as expected (see paper I and Chantereau *et al.*, in prep.), the RGB-tip is fainter for He-enriched models, therefore the maximum helium enrichment and the temperature spread decreases as we go to higher luminosities.

4. Synthetic globular clusters

4.1. *Initial conditions and basic assumptions*

The construction of a synthetic GC is based on the grid of models (see paper I) assuming a initial mass function (IMF) and an initial distribution for the initial helium mass fraction of the stars populating the cluster. We use a Paresce & De Marchi (2000) IMF for masses below $0.85\ M_\odot$, and a Salpeter IMF (Salpeter 1955) with $\alpha = 2.35$ for higher masses. The distribution of the initial helium distribution is build to retrieve the sodium distribution of the bright RGB stars of NGC 6752 (Carretta, 2013), a GC which metallicity is close to the one of our grid ([Fe/H] = -1.56, Carretta *et al.* 2009a). Indeed from the sodium abundance we can infer the helium content thanks to the helium-sodium correlation provided by the FRMS scenario (see fig. 1 in the paper I). Then with Monte-Carlo simulations of 300'000 stars (0.3 - 1.0 $M_\odot$), by iteration on the Y_{ini} distribution we reproduce this sodium distribution observed on the RGB at 13 Gyr (13.4±1.1 Gyr for NGC 6752, Gratton *et al.* 2003).

The initial helium mass fraction distribution inferred this way (see fig. 2) is composed of 49 % of stars displaying an initial helium enrichment above 0.3 and 21 % above 0.4†. After 13 Gyr, from the initial sample of 300'000 stars, only 200'000 stars (M = 0.30 - 0.81 $M_\odot$) are still alive.

4.2. *Helium distribution along the HRD at 13 Gyr*

In this section we present the distribution of stars according to their helium content at birth (Y_{ini}) and after 13 Gyr of evolution. This is shown in fig. 3 where we present the relative number of stars as a function of their initial helium content, for different regions of the HRD.

Along the MS (here $-0.5 \leqslant \log\left(\frac{L}{L_\odot}\right) \leqslant 0.3$; top panel in fig. 3), the highest initial helium content that we obtain is 0.724, which implies in principle a broadening of the MS band in the HRD by about 1,900 K. However in this domain in luminosity, only 28 % of the main sequence stars were born with Y_{ini} between 0.3 and 0.4, 11 % with Y_{ini} higher than 0.4, and 2 % with Y_{ini} higher than 0.6. Therefore, the photometric impact of the

† We used a grid of standard stellar models for low-mass stars (0.3-1.0 $M_\odot$) at low metallicity ([Fe/H] = -1.75), with an alpha-enhancement of +0.3 and initial mass fraction of helium between 0.248 and 0.8 (paper I)
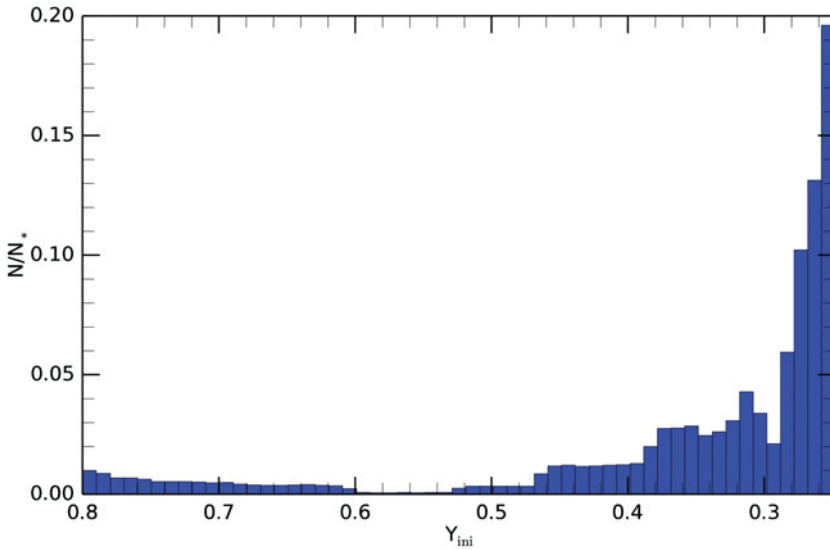
Figure 2. Initial distribution of the helium mass fraction for our sample of 300'000 stars with assumptions described in § 4.1.

high helium tail ($Y_{ini} > 0.4$) would be extremely moderate.

On the bright part of the RGB ($\log\left(\frac{L}{L_\odot}\right) \geqslant 1.2$; third panel in fig. 3, upper RGB), the maximum Y_{ini} found is nearly the same as on the MS (0.729), and the proportion of stars born with a Y_{ini} above 0.3 is 38 %, similar to the one found for the MS. In this luminosity domain, only 10 % of the stars were born with an initial helium content above 0.4, and 2 % with Y_{ini} higher than 0.6.

The RGB-tip being fainter for stars with higher initial helium content (see fig 1), as we go to higher luminosities, the maximum Y_{ini} and the fraction of present He-rich stars drops quickly, therefore the distribution of helium on the RGB is very sensitive to the bin of luminosity chosen.

At 13 Gyr all the stars with an initial helium content above 0.41 evolve directly towards the cooling white dwarf curve without undergoing the He-flash and end their life as He-WD. Therefore we do not expect to see stars born with a higher helium content on the horizontal branch (HB) and *a fortiori* on the AGB (see Charbonnel *et al.* 2013). A star with a $Y_{ini} = 0.41$ have also the lower mass on this phase (0.473 M$_\odot$) while the 1P stars on this phase have a current mass of 0.6 M$_\odot$. We also expect to still find 37 % of stars born with a helium content above 0.3 Y_{ini} but only 3 % with a helium value between 0.38 and 0.41.

Surprisingly, we find that the maximum Y_{ini} for stars on the HB is similar to the maximum He enrichment for 2P stars in the AGB scenario (~ 0.38, e.g. Doherty *et al.* 2014). Therefore we see that the determination of He for HB stars can not help discriminating between the two scenarios.

Concerning the AGB phase, the maximum Y_{ini} value found is even lower due to stars that ignite helium later on the HB (hot and late-hot flashers, see e.g. Miller Bertolami *et al.* 2008), and that miss the AGB phase, the so-called AGB-manqué stars (see e.g.
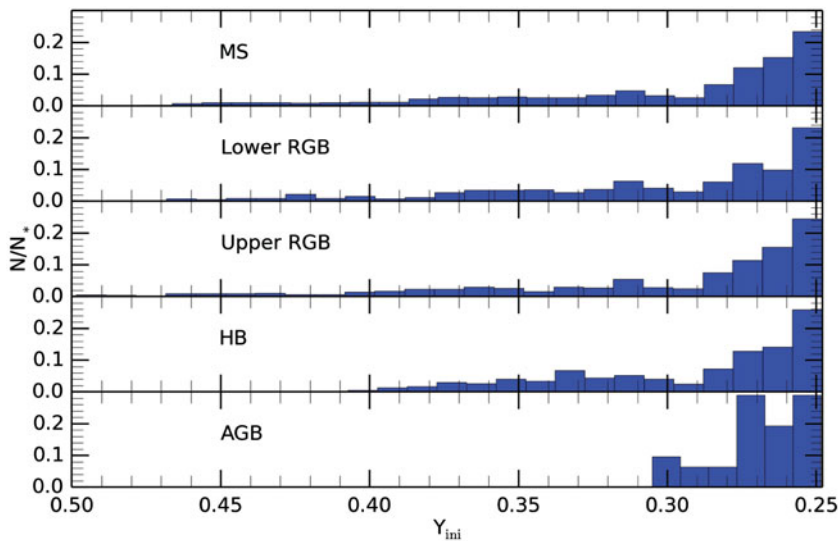
Figure 3. Y_{ini} distribution along a GC at 13 Gyr. The MS corresponds to a bin of luminosity between $\log\left(\frac{L}{L_\odot}\right) = -0.5$ and 0.3, The RGB phase is separated in two parts, the lower one displays the distribution for a bin of luminosity between $\log\left(\frac{L}{L_\odot}\right) = 0.8$ and 1.2 while the upper part shows all the brighter stars.

Charbonnel *et al.* 2013, Cassisi *et al.* 2014). At 13 Gyr, the most helium enriched model displays an initial helium content of 0.305 and a mass of 0.536 $M_\odot$ whereas its 1P counterpart has a mass of 0.598 $M_\odot$. The maximal Y_{ini} value is very sensitive to the initial helium mass fraction distribution coupled to the IMF because of the very low number of stars at this phase (31 out of the 200'000 here).

5. Conclusion

Starting with initial helium abundances for 2P stars as given by the FRMS models and using standard assumptions for the IMF, we present predictions for the helium distribution in a typical 13 Gyr old GC with [Fe/H] = -1.75.

At birth, 49 % of the stars have a helium content above 0.3, among which 21 % have Y_{ini} higher than 0.4. At 13 Gyr, due to stellar evolution, the stars born with $Y_{ini} \geqslant 0.3$ correspond to 39 % of the stars present in the GC (sum over all the phases) among which only 10 % born with a $Y_{ini} \geqslant 0.4$.

The low fraction of stars with very high helium enrichments (or their total absence) shows that it would be complicated (or impossible) to use the maximum helium enrichment as a strong discriminating parameter between the different scenarios trying to explain this multiple populations phenomenon (for this typical age and metallicity).

References

Bastian, N., Lamers, H. J. G. L. M., de Mink, S. E., Longmore, S. N., Goodwin, S. P., & Gieles, M. 2013, *MNRAS*, 436, 2398

Bedin, L. R., Piotto, G., Anderson, J., Cassisi, S., King, I. R, Momany, Y., & Carraro, G. 2004, *ApJ*, 605, L125

Carretta, E., Bragaglia, A., Gratton, R. G., Lucatello, S., Catanzaro, G., Leone, F., Bellazzini, M., Claudi, R., D'Orazi, V., Momany, Y., *et al.* 2009a, *A&A*, 505, 117

Carretta, E., Bragaglia, A., Gratton, R., D'Orazi, V., & Lucatello, S. 2009b, *A&A*, 508, 695C

Carretta, E., Bragaglia, A., Gratton, R. G., Recio-Blanco, A., Lucatello, S., D'Orazi, V., & Cassisi, S. 2010, *A&A*, 516, A55

Carretta, E. 2013, *A&A*, 557, A128

Cassisi, S., Salaris, M., Pietrinferni, A., Vink, J. S., & Monelli, M. 2014, *A&A*, 571, 81C

Chantereau, W., Charbonnel, C., & Decressin, T. 2015, *A&A*, 578, A117

Charbonnel, C., Chantereau, W., Decressin, T., Meynet, G., & Schaerer, D. 2013, *A&A*, 557, L17

Decressin, T., Charbonnel, C., & Meynet, G. 2007a, *A&A*, 475, 859

Decressin, T., Meynet, G., Charbonnel, C., Prantzos, N., & Ekström, S. 2007b, *A&A*, 464, 1029

de Mink, S. E., Pols, O. R., Langer, N., & Izzard, R. G. 2009, *A&A*, 507, L1

Denissenkov, P. A. & Hartwick, F. D. A. 2014, *MNRAS*, 437, L21

Doherty, C. L., Gil-Pons, P., Lau, H. H. B., Lattanzio, J. C., Siess, L., & Campbell, S. 2014, *MNRAS*, 441, 582

Gratton, R. G., Bonifacio, P., Bragaglia, A., Carretta, E., Castellani, V., Centurion, M., Chieffi, A., Claudi, R., Clementini, G., D'Antona, F., *et al.* 2001, *A&A*, 369, 87

Gratton, R. G., Bragaglia, A., Carretta, E., Clementini, G., Desidera, S., Grundahl, F., & Lucatello, S. 2003 *A&A*, 408, 529

Krause, M., Charbonnel, C., Decressin, T., Meynet, G., & Prantzos, N. 2013, *A&A*, 552, A121

Miller Bertolami, M. M., Althaus, L. G., Unglaub, K., & Weiss, A. 2008, **A&A** 491, 253

Milone, A. P., Marino, A. F., Piotto, G., Bedin, L. R., Anderson, J., Aparicio, A., Bellini, A., Cassisi, S., D'Antona, F., Grundahl, F., Monelli, M., & Yong, D. 2013, *ApJ*, 767, 120

Paresce, F. & De Marchi, G. 2000, *ApJ*, 534, 870

Piotto, G., Bedin, L. R., Anderson, J., King, I. R., Cassisi, S., Milone, A. P., Villanova, S., Pietrinferni, A., & Renzini, A. 2007, *ApJ*, 661, L53

Piotto, G. 2009, *IAUS*, 258, 233P

Salaris, M., Riello, M., Cassisi, S., & Piotto, G. 2004, *A&A*, 420, 911S

Salpeter, E. E. 1955, *ApJ*, 121, 161

Ventura, P., D'Antona, F., Mazzitelli, I., & Gratton, R. 2001, *ApJ*, 550, L65

Ventura, P., Di Criscienzo, M., Carini, R., & D'Antona, F. 2013, *MNRAS*, 431, 3642